Characterization of phosphorus species in sediments from the Arabian Sea oxygen minimum zone: combining sequential extractions and X-ray spectroscopy

Peter Kraal[1*], Benjamin C. Bostick[2], Thilo Behrends[1], Gert-Jan Reichart[1,3], Caroline P. Slomp[1]

[1] Department of Earth Sciences – Geochemistry, Faculty of Geosciences, Utrecht University, Budapestlaan 4, P.O. Box 80.021, 3508 TA Utrecht, The Netherlands

[2] Lamont-Doherty Earth Observatory, Earth Institute at Columbia University, 131 Comer Building, Geochemistry, 61 Route 9W, PO Box 1000, Palisades, New York 10964, USA

[3] NIOZ Royal Netherlands Institute for Sea Research, 1790AB Den Burg, Texel, The Netherlands

[*] Corresponding author, email: p.kraal@uu.nl, tel: 0031-30-2535016

ABSTRACT

The bulk phosphorus (P) distribution in sediment samples from the oxygen minimum zone of the northern Arabian Sea was determined using two methods: sequential chemical extraction (the 'SEDEX' procedure) and X-ray absorption near-edge structure (XANES) spectroscopy of the phosphorus K-edge. Our results show good agreement between iron (Fe-)associated P and calcium phosphate minerals (Ca-P) determined by both methods. Furthermore, we find that SEDEX exchangeable P likely represents loosely Fe-bound P, and that the SEDEX detrital fraction may consist partly of polyphosphate, i.e. microbially synthesized intracellular phosphate. Below productive waters with relatively high sedimentary organic matter and P contents, polyphosphates may represent an important P sink that is not easily identified by chemical sequential extraction. This study highlights the value of SEDEX as a generally accurate and fast P speciation technique (especially for Fe- and Ca- P) and, for the first time, demonstrates the possibilities of P K-edge XANES as a bulk P speciation tool for marine sediments.

Keywords: phosphorus speciation, marine sediments, sequential extraction, SEDEX, X-ray absorption spectroscopy

1. Introduction

Burial in sediments is the only long-term sink for the essential nutrient phosphorus (P) in the marine environment. During burial, microbial decomposition and reductive dissolution processes lead to the partial release of P from labile reservoirs such as organic matter (OM), fish bones and ferric iron (Fe) (oxyhydr)oxides into the pore-water. This released P (typically HPO_4^{2-}) either diffuses from the sediment to the overlying seawater or precipitates in authigenic calcium phosphate minerals (Ca-P), generally as carbonate fluorapatite: $Ca_5(PO_4)_{3-x}(CO_3)_x(OH,F)$ (Froelich et al., 1982). The conversion of labile P phases to stable authigenic Ca-P constitutes the principal long-term burial mechanism for P in marine sediments (Ruttenberg and Berner, 1993; Slomp et al., 1996a; Anderson et al., 2001). Detrital P, i.e. P associated with detrital grains that sink to the seafloor and do not represent a sink for or source of bio-available P, is another potentially important P reservoir in marine sediments. Quantifying labile and stable authigenic P pools as well as detrital P phases is important for understanding marine P cycling and bio-availability. Additionally, the chemical forms of P in sediments are a function of redox conditions and can be used to reconstruct depositional conditions from sedimentary records; Fe(III)-associated P is generally scarce in reducing sediments, and reducing sediments facilitate more efficient regeneration of P from organic matter compared to oxic sediments (Ingall et al., 1993; Kraal et al., 2010; Jilbert et al., 2011).

Determining P phases in marine sediments has so far mostly depended on sequential chemical extraction methods adapted from P studies in lakes, rivers and soils (Lucotte and d'Anglejan, 1985; Ruttenberg, 1992; Jensen and Thamdrup, 1993). The 'SEDEX' sequential extraction procedure, developed by Ruttenberg (1992) and validated using a suite of common marine organic and inorganic P phases, has been particularly successful. The extraction scheme separates five operationally-defined P phases: (1) exchangeable P, (2) ferric Fe-

associated P, (3) authigenic, biogenic and $CaCO_3$-bound P, (4) detrital P and (5) organic P (see Table 1 for full description of extraction steps). Nevertheless, various studies have highlighted the potential limitations of operationally-defined extractions. For instance, Anderson and Delaney (2000) suggested that exchangeable P consists predominantly of loosely Fe-bound P and therefore proposed to omit step 1 of the original SEDEX procedure. Furthermore, separation of authigenic and detrital P minerals in ancient sediments may be complicated by the crystallization of authigenic Ca-P, which results in recalcitrant apatite that is extracted as detrital P rather than authigenic Ca-P (Anderson et al., 2001; Föllmi et al., 2005). Alternatively, relatively labile detrital P may be dissolved together with (and incorrectly characterized as) authigenic Ca-P (Kraal et al., 2012). Lastly, it has been shown that the reducing citrate-bicarbonate-dithionite solution used to extract P associated with ferric Fe minerals may partially dissolve labile P phases such as biogenic apatite and vivianite (Williams et al., 1980; Nembrini et al., 1983; Selig and Fischer, 2005). In conclusion, care should be taken when directly interpreting results of sequential extractions as a quantitative measure of chemical forms of P in sediments

Another method to characterize P species in marine samples is ^{31}P nuclear magnetic resonance (NMR). Solid-state and solution ^{31}P NMR studies have provided detailed insight into P speciation in sinking marine particulate matter and marine sediments, particularly for organic P compounds (Paytan et al., 2003; Cade-Menun et al., 2005; Sannigrahi and Ingall, 2005). Nevertheless, solid-state NMR suffers from interference by paramagnetic ions such as Fe and Mn. Solution ^{31}P NMR increases spectral resolution, thus enabling the identification of specific inorganic P phases, but requires selective sample extractions that can affect P speciation (Cade-Menun et al., 2005).

An important advance has been the use of synchrotron-based X-ray absorption near-edge structure (XANES) spectroscopy of the phosphorus K-edge to determine P speciation in soil

and sediment samples (Beauchemin et al., 2003; Sato et al., 2005; Brandes et al., 2007; Diaz et al., 2008; Longo et al., 2014). Detailed information on the (mineral) properties of P phases is derived from distinct spectral features of the P K-edge absorption peak, which reflect the binding environment of the absorbing atom and result from electron scattering processes (Franke and Hormes, 1995; Hesterberg et al., 1999; Myneni, 2002). Different forms of P have been distinguished based on similarities between the spectra of samples and those of well-characterized reference materials. A great advantage of this technique is that virtually no sample preparation is required for spectroscopic analysis. This avoids destruction of the original sedimentary signatures by various chemical pre-treatments.

Phosphorus speciation with P K-edge XANES has up to now mostly been applied to the study of soils, wastewater and manure (Peak et al., 2002; Beauchemin et al., 2003; Sato et al., 2005; Shober et al., 2006; Güngör et al., 2007; Kar et al., 2011; Prietzel et al., 2013). In such materials, P concentrations are sufficiently high for a quantitative statistical approach to bulk P speciation using the least squares – linear combination fitting (LCF) technique, whereby spectra of reference materials are combined to produce a model spectrum that best represents the sample spectrum. The relative contributions of the reference spectra are then used as a measure of their relative abundance in the sample (Beauchemin et al., 2003). The characteristic spectral features of a variety of P reference compounds have been discussed in detail in recent studies (Brandes et al., 2007; Ingall et al., 2011).

To date, collection of P K-edge XANES spectra in marine samples focused on microprobe measurements, whereby P K-edge XANES spectra are obtained from specific µm-scale P-rich sample regions. As such, spectra are likely to capture single P particles or phases in the sediment, allowing for qualitative P speciation by comparison to reference spectra. Using this approach, polyphosphates and Ca-P minerals have been identified in marine sediments (Brandes et al., 2007; Diaz et al., 2008). This approach, however, only provides information

on P speciation in marine samples when a large number of individual spots are analyzed (Diaz et al., 2008). Therefore, P K-edge XANES spectroscopy can potentially serve to characterize the P speciation in bulk sediment samples. Additionally, combining X-ray spectroscopy with chemical fractionation will provide insight into analytical performance as well as detailed sedimentary P speciation. Such a combined approach has been applied to soil samples (Beauchemin et al., 2003; Kar et al., 2011), but not to marine sediments.

Here, we compare P speciation as determined with SEDEX (sequential extraction) with results of P K-edge XANES (spectroscopy) analyses of freshly collected and well-preserved surface sediments from the Arabian Sea. This marine system features a permanent oxygen minimum zone (OMZ) between ~ 200 and 1200 m water depth, resulting from a combination of seasonally high productivity and sluggish circulation. Where the sea floor topography intersects the OMZ, large amounts of organic matter are buried in the sediment, leading to relatively high sedimentary P concentrations. So far, investigations into P cycling and speciation in Arabian Sea sediments have been restricted to chemical extractions (Schenau et al., 2000; Prakash Babu and Nath, 2005; Kraal et al., 2012) and our study is the first to directly compare results of chemical and spectroscopic methods to characterize chemical forms of P in marine sediments.

2. Materials and methods

2.1. Sampling area and sediment collection

During the PASOM research expedition on the R/V Pelagia in January 2009, the water column and sediment were sampled at ten stations along a depth transect from inside to below the OMZ in the Murray Ridge area of the northeastern Arabian Sea (Figure 1). Water column dissolved oxygen profiles were measured with a Seabird oxygen sensor attached to a

conductivity, temperature, depth (CTD) profiler. In addition, the top 20 – 30 cm of the sediment at each station was collected using an Oktopus multi corer. A detailed geochemical characterization of the sediments is given by Kraal et al. (2012). For this study, we used sediment cores from Station 1B and 2 which were located at the lower boundary of the OMZ (Figure 1; Table 2). Immediately after recovery, the cores with overlying bottom water were capped with rubber stoppers and transferred to a N_2-purged glovebox. After removal of the overlying bottom water, the sediment was sliced at high resolution (0.5 – 2 cm intervals, increasing with depth). For each sampling interval, a subsample of the wet sediment was directly transferred into a 15 mL glass vial, which was stored in an air-tight glass jar under oxygen-free conditions at -20 °C until further processing.

2.2. Chemical bulk solid-phase analyses

A subsample of the wet sediment was transferred to a micro-centrifuge tube in an argon-purged glove box and was stored cool in air-tight jars prior to P K-edge XANES analysis. The remaining wet sediment was freeze-dried and thoroughly ground with an agate mortar in an Ar-purged glovebox. Analyses of total organic C (C_{org}), Fe and P as well as sequential extraction of Fe and P phases were performed as detailed in Kraal et al. (2012). In short, C_{org} was measured with a CNS analyzer after decalcification of a sub sample of the freeze-dried and ground sediment with 1 M HCl. Loss of C_{org} during decalcification has been shown to be negligible (Van Santvoort et al., 2002). Total Fe and P were determined in another sub sample by total digestion in a mixture of 2.5 mL HF and 2.5 mL 3:2 $HClO_4$:HNO_3, and subsequent measurement of Fe and P by ICP-OES. Sequential extraction of Fe phases was carried out following the method proposed by Poulton and Canfield (2005), and P phases were sequentially extracted with the SEDEX procedure (Ruttenberg, 1992) as adapted by

123 Slomp et al. (1996b) but including the step for exchangeable P. The sequential extraction
124 methods are summarized in Table 1.
125
126 *2.3. Phosphorus X-ray absorption near-edge spectroscopy*

127 Phosphorus K-edge XANES spectra were collected at the National Synchrotron Light
128 Source at Brookhaven National Laboratory (Upton, New York) using beamline X19A
129 equipped with a Si(III) monochromator that operated at 0.2 eV resolution at the P K-edge.
130 The P K-edge XANES spectra were collected within one week after the research cruise.
131 Together with anoxic sample preparation, frozen storage and cooled transport, this ensured
132 that changes in the redox state of the sediment that can alter P partitioning were minimized
133 (Kraal et al., 2009; Kraal and Slomp, 2014). Spectra were collected at ambient temperature in
134 fluorescence mode using a beam size of 1 x 7 mm and a solid-state passivated implanted
135 planar silicon (PIPS) detector. The sample chamber and detector were continuously purged
136 with He to minimize the attenuation of X-rays and prevent sample oxidation during analysis.
137 Fluorescence spectra were collected between 2139 and 2174 eV with an energy step size of
138 0.2 eV and a dwell time of 2 s. The energy scale was calibrated by assigning the inflection
139 point of the first absorption peak (E_0) of the reference mineral variscite (Table 3) to an energy
140 of 2149.0 eV (Hesterberg et al., 1999). Repeated measurements of the variscite reference
141 sample during the 3-day period of data collection showed no measurable peak shift.
142 A total of 18 samples from stations 1B and 2 and a suite of reference materials (Table 3)
143 were analyzed. This selection represents samples from within the OMZ that contained
144 comparatively high concentrations of P (~ 35 – 90 μmol g^{-1}) (Kraal et al., 2012). These
145 spectra were selected from a larger set of spectra from sediments samples (~50) that were
146 recovered at various stations during the PASOM cruise in 2009. The signal-to-noise ratio

147 quickly decreased with decreasing P concentration at stations outside of the OMZ, making
148 these samples unsuitable for quantitative spectroscopic P speciation. Generally, three to six
149 spectra were collected for all reference compounds and samples. All mineral reference
150 compounds were either taken from the Dartmouth College mineral collection (DMC; verified
151 by X-ray diffraction) or were freshly synthesized in the laboratory using analytical grade
152 chemicals. The organic P reference materials, phytic acid (inositol hexakiphosphate) and
153 pentasodium tripolyphosphate, were commercially purchased. Small quantities of powdered
154 reference materials were brushed onto Kapton tape that was attached to the Plexiglas sample
155 holder. Wet sediment samples were spread as thin as possible on a Whatman No. 1 filter that
156 was attached to the sample holder. The reference materials and samples were not covered in
157 order to minimize loss of fluorescence signal. After loading the sample, the sample chamber
158 and detector were purged with He for several minutes before each measurement to minimize
159 X-ray absorption by air.
160 Normalization and least squares - linear combination fitting (LCF) were performed with
161 the Athena software package (Ravel and Newville, 2005). Final spectra of samples and
162 reference materials used in fitting were selected from either single or averaged spectra.
163 Stability of the background signal, which usually improved with sample chamber purging,
164 was the most important factor in determining the quality of the spectra and, in turn, the
165 goodness of the fits. A final set of nine sample spectra that displayed the best signal-to-noise
166 ratios was selected for LCF. To determine an appropriate set of reference materials for LCF,
167 the Athena ‘combinatorics’ function was used to fit with all combinations of reference
168 materials and assess the goodness-of-fit.
169

3. Results

3.1. SEDEX: Chemical phosphorus and iron fractionation

The organic-rich sediments from Station 1B and 2 were deposited under low-oxygen bottom water conditions (Table 2). Despite similar present-day bottom water oxygenation, there were marked differences in the chemical forms of P and Fe between the two stations (Fig. 2). The subsurface sediments (0 – 10 cm depth) at Station 1B were enriched in P, mainly present as exchangeable and Fe-associated P (together making up 35 – 60 % of total P). This P enrichment coincided with a pronounced peak in labile and crystalline Fe (oxyhydr)oxides. The relative contribution of authigenic Ca-P increased steadily down-core and accounted for 40 – 65% of total P below 10 cm sediment depth. Detrital and organic P were relatively stable throughout the core, accounting for approximately 5 % and 10 % of total P, respectively. Exchangeable P and Fe-associated P were positively correlated (R^2 = 0.85; Fig. 3a), as were authigenic P and detrital P (R^2 = 0.59; Fig. 3b).

Compared to station 1B, only little Fe-associated P was observed at station 2 (Figure 2). Labile and crystalline Fe (oxyhydr)oxides were less abundant than at Station 1B, particularly at shallow depth. Authigenic Ca-P was the major P phase throughout the investigated surface sediment, making up 50 – 75% of total P. Between ~ 15 and 26 cm depth, an increase in authigenic Ca-P and, to a lesser extent, detrital P contents was observed. Organic P decreased steadily with depth, its relative abundance dropping down-core from 20 % to 5 % of total P. In the sediment from station 2, no clear correlation was observed between exchangeable P and Fe-associated P, whereas authigenic Ca-P and detrital P were strongly correlated (R^2 = 0.93) (Fig. 3).

193 *3.2. P K-edge XANES spectroscopy*

194 Least squares – linear combination fitting (LCF) of the sample spectra with different
195 numbers of reference spectra (between 2 and 5) showed that using more than four reference
196 spectra did not increase the quality of the fit as reflected by the R-factor (Fig. 4). For each
197 sample, the set of four reference spectra that resulted in the best fit was determined. These
198 results were pooled, resulting in a final set of six standards that were used to reproduce all
199 sample spectra. (Table 4). The reference spectra could be grouped in three main groups of P
200 compounds: Fe-associated P (ferrihydrite-adsorbed PO_4 and vivianite), Ca-P (collophane and
201 fluorapatite) and organic P (polyphosphate and phytic acid). After LCF, the relative
202 abundance of each of these groups (Fe-associated P, Ca-P, organic P) was calculated by
203 summing the fractions of the two reference materials within each group. This allowed for
204 better comparison between SEDEX and P K-edge XANES. The ferrihydrite-adsorbed PO_4
205 (Fh-PO_4) and vivianite reference materials represent phosphate adsorbed onto Fe
206 (oxyhydr)oxides and Fe phosphate minerals, respectively. Polyphosphate is treated as organic
207 P since it forms through microbial intracellular P sequestration in sediments (Schulz and
208 Schulz, 2005; Diaz et al., 2008).

209 Several authors discussed the spectral properties of a variety of phosphorus reference
210 materials in detail (Hesterberg et al., 1999; Brandes et al., 2007; Ingall et al., 2011). Here, we
211 focus exclusively on the spectral properties of sediment samples and relevant reference
212 materials (Fig. 5). The Fe-associated P reference materials were characterized by a pre-edge
213 feature and a relatively high energy for the absorbance peak compared to Ca-P reference
214 materials. The latter were set apart from all other P phases by a distinct post-edge shoulder.
215 The phytic acid and polyphosphate spectra showed a relatively broad absorption peak, with
216 maxima at energies similar to the absorption peak of Fe-associated P reference materials. The

P K-edge XANES spectra of station 1B samples showed a change between sample 3 (4.5 cm) and 4 (11 cm depth): the deeper samples showed a negative energy shift of ~ 1 eV of the peak position and a post-edge shoulder feature. The energy of the absorption peak is similar to that of the Fe-associated P reference materials for the top three samples, and similar to that of the Ca-P reference materials for the bottom two samples. The absorption peaks of the P K-edge XANES spectra of station 2 samples all have energies similar to those of the deeper station 1B samples. The most notable change with depth at station 2 is the development of a more pronounced shoulder feature on the high-energy side of the absorption peak.

Overall, the P K-edge XANES results agreed with the SEDEX results in showing a transition with depth from Fe-associated P to Ca-P as the dominant P pool at station 1B (Table 5), and a strong correlation between these two P pools as measured by chemical extraction and X-ray spectroscopy (Fig. 6). A better correlation between SEDEX and P K-edge XANES results was obtained when the sum of SEDEX Fe-associated P and exchangeable P was plotted against Ca-P as determined by P K-edge XANES (Fig 7a). The organic P fractions determined by LCF of P K-edge XANES spectra were more weakly correlated to the SEDEX results (Table 5, Fig. 6c). Here, a better correlation was obtained when the sum of SEDEX organic P and detrital P was plotted against organic P as determined by P K-edge XANES, in particular for station 2.

Estimates of the relative contribution of individual reference materials to the major P species (Fe-associated P, Ca-P and organic P) found in four different sediment depth intervals are shown in Fig. 7. An Fe phosphate as represented by the vivianite reference spectrum was the dominant Fe-associated P component, except at 4.5 and 11 cm sediment depth, where the SEDEX results showed enrichment in Fh-PO_4. With regards to Ca-P, the collophane component accounted for a relatively large proportion of Ca-P at station 2 compared to station 1B. No clear trends in speciation within the organic P group were observed.

4. Discussion

4.1. Spectroscopic differentiation between phosphorus reference materials

Phosphorus in natural mineral and organic compounds occurs predominantly in the form of P(+V). As a consequence, P K-edge XANES spectra of various P compounds are similar and spectroscopic identification of individual P compounds is challenging. Nevertheless, there are certain defining features for P species that allow for distinguishing between P species (for detailed overview see: Franke and Hormes, 1995; Brandes et al., 2007; Ingall et al., 2011). With respect to the P reference materials used in this study, Fe-associated P and Ca-P compounds are differentiated by several spectral features (Fig. 5): (i) a pre-edge feature for Fe-associated P, (ii) a distinct post-edge shoulder for Ca-P, and (iii) an energy difference for the absorption peaks of approximately 0.5 eV. The other P reference materials, phytic acid and pentasodium tripolyphosphate, generally lack distinct pre- or post-edge features, and are characterized by relatively broad absorption peaks that lie at the same energy as those of the Fe-associated P reference spectra. In the case of polyphosphate, the shape of the spectrum around 2149 eV suggests a split peak which has been associated with the formation of bridging P-O-P units, resulting in different unoccupied electronic states (Franke and Hormes, 1995). A split peak is not always observed in the XANES P K-edge spectra of polyphosphates (Diaz et al., 2008). Whereas the spectra of phytic acid and polyphosphate are easily distinguished from Fe-associated P and Ca-P reference materials (Fig. 5), their relatively featureless broad absorption peaks may complicate their identification in complex mixtures of P species that occur in natural samples. This is further discussed in section 4.3.

4.2. Combining sequential extraction and P K-edge XANES spectroscopy for phosphorus speciation

In this study, we aimed to investigate the partitioning of P among various phases in sediments by analyzing bulk samples with X-ray spectroscopy as well as performing sequential chemical extractions. Because differences between P K-edge XANES spectra of P reference materials within the same class (e.g. Fe-associated P and Ca-P) are relatively small (see also section 4.1), we first investigate the relationships between main P phases as quantified by sequential extraction and P K-edge XANES spectroscopy: Fe-associated P, Ca-P and P associated with organic matter. Because detrital P is generally made up of a mixture of recalcitrant P phases, it is not easily assigned to a specific P reference material for P K-edge XANES and therefore is not considered separately.

There is good agreement between Fe-associated P and Ca-P as determined by chemical extraction and spectroscopy (Fig. 6a and b). Moreover, P K-edge XANES provides further insight into the nature of the operationally-defined P pools targeted by the chemical extraction. The apparent underestimation of Fe-associated P by SEDEX at high relative abundances of this P phase decreases when exchangeable P is included in the Fe-associated P pool, suggesting that P extracted during the first step is loosely bound to Fe (oxyhydr)oxides. This has been hypothesized before for marine sediments (Anderson and Delaney, 2000), but our combined approach provides empirical evidence. The underestimation of Ca-P by P K-edge XANES relative to SEDEX at low relative abundances may reflect the inability of P K-edge XANES spectroscopy to accurately quantify low concentrations of Ca-P. Likewise, the fact that the x intercept in the scatter plot of XANES vs SEDEX Fe-associated P lies around 0.1 (Fig. 6a) suggests that low relative abundances of Fe-associated P were not detected by LCF of P K-edge XANES spectra. In this regard, we note that O'Day et al. (2004) showed

that Fe species with a relative abundance of less than 5 % of total Fe are not detectable in the X-ray spectra of simple mixtures of Fe phases (consisting of Fe-rich clay and pyrite in a quartz matrix). In the investigated sediments, with P concentrations around 50 µmol g^{-1} (orders of magnitude lower than common sedimentary Fe concentrations, which amount to several wt%), the positive x intercepts in Fig. 6a and b suggest that the lower limit for identification of P phases with P K-edge XANES spectroscopy lies around 10 - 20 % of total P.

The organic P, as determined by P K-edge XANES spectroscopy, was relatively high compared to the SEDEX results for various sediment samples (Fig. 6c). This may be attributed to the fact that LCF was performed with reference materials that represent three groups of P compounds: Ca-P, Fe-associated P and organic P. The latter was represented by reference spectra that lacked distinct features (Fig. 5). The 'organic' P pool as determined by P K-edge XANES may then represent a residual pool of P phases not identified as Fe-associated P or Ca-P during LCF. This may cause an overestimation of organic P compared to SEDEX, which separates this residual pool into organic P and detrital P.

Despite these challenges, the combined use of SEDEX and P K-edge XANES may provide further insight into the nature of detrital P pools obtained from the SEDEX extraction. The good agreement between SEDEX and P K-edge XANES for Ca-P suggests that the detrital P pool is unlikely to contain much crystallized Ca-P. Following a similar logic for Fe-associated P, the detrital P pool is expected to contain little Fe-associated P. With Ca-P and Fe-associated P ruled out as major contributors to the SEDEX detrital P fraction, our results suggest that polyphosphates and organic P (here represented by phytic acid) may be important components of the residual P pool that is differentiated into detrital and organic P by the SEDEX procedure. Together with observations reported in other studies (Diaz et al., 2008; Björkman, 2014), this implies that polyphosphates can be an important sedimentary P

pool under a variety of marine settings, from nutrient-depleted to relatively nutrient-rich waters such as the Arabian Sea upwelling area investigated here. Furthermore, polyphosphates associated with microbial cells can be extracted with 1 M HCl (Eixler et al., 2005) and subsequently misconstrued as detrital P during sequential chemical extraction. We emphasize, however, that distinguishing between various organic P phases is challenging. This is illustrated in Fig. 7c, which shows seemingly random variability in the relative distribution of polyphosphate and phytic acid. Therefore, complementary techniques such as ^{31}NMR would be required for a detailed study of the organic P component.

Finally, we explore to what extent the P K-edge XANES results inform us on the nature of P compounds within the classes of Fe-associated P and Ca-P. In the case of Ca-P, the (carbonate) fluorapatite and collophane standards used in this study cannot be separated based on chemical structure, as both minerals are described as $Ca_5(PO_4,CO_3)_3F$. Collophane is cryptocrystalline fluorapatite, which is expressed by a more pronounced absorption peak and less features in the post-edge region (Fig. 5). The post-edge shoulder is known to become less distinctive with decreasing crystallinity of Ca-P (Sato et al., 2005; Oxman, 2013). Due to difficulties in discerning between different Ca-P phases, especially when using a small set of reference materials and natural sediment samples, we will not attempt to interpret the relative distributions of fluorapatite and collophane in any detail. Whereas a similar problem with regard to the similarity of spectral features arises for Fe-associated P (Fig. 5), there is good agreement between the spectroscopic and chemical results: the relative contribution of the Fh-PO_4 component is by far the highest (Fig. 7a) in the two samples from the sediment interval with a strong enrichment in Fe (oxyhydr)oxides and Fe-bound P (Fig. 2). Iron-associated P in this interval may indeed predominantly exist as phosphate adsorbed to fresh Fe (oxyhydr)oxides, whereas other samples may mostly contain Fe-associated P in the form of an Fe-P mineral (represented by the vivianite reference material in this study). This could

reflect P diagenesis under the anoxic and non-sulfidic conditions that prevail in Arabian Sea OMZ surface sediments, from active adsorption onto freshly precipitated Fe in surface sediments to formation of (reduced) Fe-associated P minerals at depth, as a result of reductive dissolution-precipitation reactions.

5. Conclusions

Our P K-edge XANES results confirm the reliability of the SEDEX procedure to determine Fe-associated P and Ca phosphate minerals, where the latter may consist of both authigenic and detrital phases. Furthermore, the combination of sequential chemical extractions using SEDEX and P K-edge XANES spectroscopy can provide further insight into the nature of the operationally-defined P phases. Our results suggest that polyphosphates, which can be misconstrued as detrital P based on chemical extraction, may be a quantitatively important P pool in sediments underlying productive surface waters.

Acknowledgments

The Netherlands Organisation for Scientific Research is acknowledged for financial support to P. Kraal and C.P. Slomp (NWO Vidi grant 86405.004 and Open Competition Grant 822.01013). C.P. Slomp acknowledges funding by the European Research Council under the European Community's Seventh Framework Programme for ERC Starting Grant #278364. G.J Reichart acknowledges the Earth and Life Sciences (ALW) division of the Netherlands Organisation for Scientific Research (NWO)NWO for funding the 2009 PASOM research expedition. The shipboard party on the R/V Pelagia is thanked for their logistic and analytical support during the 2009 PASOM expedition. Use of the National Synchrotron Light Source (NSLS), Brookhaven National Laboratory, was supported by the U.S.

Department of Energy, Office of Science, Office of Basic Energy Sciences. NSLS scientists at beamline X19A are gratefully acknowledged for their help and support during collection of P K-edge XANES spectra. S.W. Poulton at Newcastle University contributed to the sequential Fe extractions performed on the samples from Station 2. We thank the staff of the Utrecht University integrated lab for the ICP-OES measurements.

References

Anderson, L.D., Delaney, M.L., 2000. Sequential extraction and analysis of phosphorus in marine sediments: Streamlining of the SEDEX procedure. Limnol. Oceanogr. 45, 509-515.

Anderson, L.D., Delaney, M.L., Faul, K.L., 2001. Carbon to phosphorus ratios in sediments: Implications for nutrient cycling. Global Biogeochem. Cy. 15, 65-79.

Beauchemin, S., Hesterberg, D., Chou, J., Beauchemin, M., Simard, R.R., Sayers, D.E., 2003. Speciation of phosphorus in phosphorus-enriched agricultural soils using X-Ray absorption near-edge structure spectroscopy and chemical fractionation. J. Environ. Qual. 32, 1809-1819.

Brandes, J.A., Ingall, E., Paterson, D., 2007. Characterization of minerals and organic phosphorus species in marine sediments using soft X-ray fluorescence spectromicroscopy. Mar. Chem. 103, 250-265.

Cade-Menun, B.J., Benitez-Nelson, C.R., Pellechia, P., Paytan, A., 2005. Refining ^{31}P nuclear magnetic resonance spectroscopy for marine particulate samples: Storage conditions and extraction recovery. Mar. Chem. 97, 293-306.

Cowie, G.L., Levin, L.A., 2009. Benthic biological and biogeochemical patterns and processes across an oxygen minimum zone (Pakistan margin, NE Arabian Sea). Deep-Sea Res. Pt. II 56, 261-270.

Diaz, J., Ingall, E., Benitez-Nelson, C., Paterson, D., de Jonge, M.D., McNulty, I., Brandes, J.A., 2008. Marine polyphosphate: A key player in geologic phosphorus sequestration. Science 320, 652-655.

Eixler, S., Selig, U., Karsten, U., 2005. Extraction and detection methods for polyphosphate storage in autotrophic planktonic organisms. Hydrobiologia 533, 135-143.

Föllmi, K.B., Badertscher, C., De Kaenel, E., Stille, P., John, C.M., Adatte, T., Steinmann, P., 2005. Phosphogenesis and organic-carbon preservation in the Miocene Monterey Formation at Naples Beach, California--The Monterey hypothesis revisited. Geol. Soc. Am. Bull. 117, 589-619.

Franke, R., Hormes, J., 1995. The P K-near edge absorption spectra of phosphates. Physica B: Condensed Matter 216, 85-95.

Froelich, P.N., Bender, M.L., Luedtke, N.A., Heath, G.R., DeVries, T., 1982. The marine phosphorus cycle. Am. J. Sci. 282, 474-511.

Güngör, K., Jurgensen, A., Karthikeyan, K.G., 2007. Determination of phosphorus speciation in dairy manure using XRD and XANES spectroscopy. J. Environ. Qual. 36, 1856-1863.

Hesterberg, D., Zhou, W., Hutchison, K.J., Beauchemin, S., Sayers, D.E., 1999. XAFS study of adsorbed and mineral forms of phosphate. J. Synchrotron Radiat. 6, 636-638.

Ingall, E.D., Brandes, J.A., Diaz, J.M., de Jonge, M.D., Paterson, D., McNulty, I., Elliott, W.C., Northrup, P., 2011. Phosphorus K-edge XANES spectroscopy of mineral standards. J. Synchrotron Radiat. 18, 189-197.

Ingall, E.D., Bustin, R.M., Van Cappellen, P., 1993. Influence of water column anoxia on the burial and preservation of carbon and phosphorus in marine shales. Geochim. Cosmochim. Acta 57, 303-316.

Jensen, H., Thamdrup, B., 1993. Iron-bound phosphorus in marine sediments as measured by bicarbonate-dithionite extraction. Hydrobiologia 253, 47-59.

Jilbert, T., Slomp, C.P., Gustafsson, B.G., Boer, W., 2011. Beyond the Fe-P-redox connection: preferential regeneration of phosphorus from organic matter as a key control on Baltic Sea nutrient cycles. Biogeosciences 8, 1699-1720.

Kar, G., Hundal, L.S., Schoenau, J.J., Peak, D., 2011. Direct chemical speciation of P in sequential chemical extraction residues using P K-Edge X-Ray absorption near-edge structure spectroscopy. Soil Sci. 176, 589-595 510.1097/SS.1090b1013e31823939a31823933.

Kraal, P., Slomp, C.P., 2014. Rapid and extensive alteration of phosphorus speciation during oxic storage of wet sediment samples. PLoS ONE 9, e96859.

Kraal, P., Slomp, C.P., de Lange, G.J., 2010. Sedimentary organic carbon to phosphorus ratios as a redox proxy in Quaternary records from the Mediterranean. Chem. Geol. 277, 167-177.

Kraal, P., Slomp, C.P., Forster, A., Kuypers, M.M.M., Sluijs, A., 2009. Pyrite oxidation during sample storage determines phosphorus fractionation in carbonate-poor anoxic sediments. Geochim. Cosmochim. Acta 73, 3277-3290.

Kraal, P., Slomp, C.P., Reed, D.C., Reichart, G.J., Poulton, S.W., 2012. Sedimentary phosphorus and iron cycling in and below the oxygen minimum zone of the northern Arabian Sea. Biogeosciences 9, 2603-2624.

Longo, A.F., Ingall, E.D., Diaz, J.M., Oakes, M., King, L.E., Nenes, A., Mihalopoulos, N., Violaki, K., Avila, A., Benitez-Nelson, C.R., Brandes, J., McNulty, I., Vine, D.J., 2014. P-NEXFS analysis of aerosol phosphorus delivered to the Mediterranean Sea. Geophys. Res. Lett., 41: 2014GL060555.

Lucotte, M., d'Anglejan, B., 1985. A comparison of several methods for the determination of iron hydroxides and associated orthophosphates in estuarine particulate matter. Chem. Geol. 48, 257-264.

Myneni, S.C.B., 2002. Soft X-ray spectroscopy and spectromicroscopy studies of organic molecules in the environment. Rev. Mineral. Geochem. 49, 485-579.

Nembrini, G.P., Capobianco, J.A., Viel, M., Williams, A.F., 1983. A Mössbauer and chemical study of the formation of vivianite in sediments of Lago Maggiore (Italy). Geochim. Cosmochim. Acta 47, 1459-1464.

O'Day, P.A., Rivera, N., Root, R., Carroll, S.A., 2004. X-ray absorption spectroscopic study of Fe reference compounds for the analysis of natural sediments. Am. Mineral. 89, 572-585.

Oxman, J.F., 2013. An X-ray absorption method for the identification of calcium phosphate species using peak height ratios. Biogeosciences Discussions 10, 18723–18756.

Paytan, A., Cade-Menun, B.J., McLaughlin, K., Faul, K.L., 2003. Selective phosphorus regeneration of sinking marine particles: evidence from ^{31}P-NMR. Mar. Chem. 82, 55-70.

Peak, D., Sims, J.T., Sparks, D.L., 2002. Solid-state speciation of natural and alum-amended poultry litter using XANES spectroscopy. Environ. Sci. Technol. 36, 4253-4261.

Poulton, S.W., Canfield, D.E., 2005. Development of a sequential extraction procedure for iron: implications for iron partitioning in continentally derived particulates. Chem. Geol. 214, 209-221.

Prakash Babu, C., Nath, B.N., 2005. Processes controlling forms of phosphorus in surficial sediments from the eastern Arabian Sea impinged by varying bottom water oxygenation conditions. Deep-Sea Res. Pt. II 52, 1965-1980.

Prietzel, J., Dümig, A., Wu, Y., Zhou, J., Klysubun, W., 2013. Synchrotron-based P K-edge XANES spectroscopy reveals rapid changes of phosphorus speciation in the topsoil of two glacier foreland chronosequences. Geochim. Cosmochim. Acta 108, 154-171.

Ravel, B., Newville, M., 2005. Athena, Artemis, Hephaestus: data analysis for X-ray absorption spectroscopy using IFEFFIT. J. Synchrotron Radiat. 12, 537-541.

Ruttenberg, K.C., 1992. Development of a sequential extraction method for different forms of phosphorus in marine sediments. Limnol. Oceanogr. 37, 1460-1482.

Ruttenberg, K.C., Berner, R.A., 1993. Authigenic apatite formation and burial in sediments from non-upwelling, continental-margin environments. Geochim. Cosmochim. Acta 57, 991-1007.

Sannigrahi, P., Ingall, E., 2005. Polyphosphates as a source of enhanced P fluxes in marine sediments overlain by anoxic waters: Evidence from ^{31}P NMR. Geochem. T. 6, 52-59.

Sato, S., Solomon, D., Hyland, C., Ketterings, Q.M., Lehmann, J., 2005. Phosphorus speciation in manure and manure-amended soils using XANES spectroscopy. Environ. Sci. Technol. 39, 7485-7491.

Schenau, S.J., Slomp, C.P., De Lange, G.J., 2000. Phosphogenesis and active phosphorite formation in sediments from the Arabian Sea oxygen minimum zone. Mar. Geol. 169, 1-20.

Schulz, H.N., Schulz, H.D., 2005. Large sulfur bacteria and the formation of phosphorite. Science 307, 416-418.

Selig, U., Fischer, K., 2005. Phosphorus accumulation in lake sediments during the last 14,000 years: Description by fractionation techniques and X-ray micro-analysis. J. Freshwater Ecol. 20, 347-359.

Shober, A.L., Hesterberg, D.L., Sims, J.T., Gardner, S., 2006. Characterization of phosphorus species in biosolids and manures using XANES spectroscopy. J. Environ. Qual. 35, 1983-1993.

Slomp, C.P., Epping, E.H.G., Helder, W., Van Raaphorst, W., 1996a. A key role for iron-bound phosphorus in authigenic apatite formation in North Atlantic continental platform sediments. J. Mar. Res. 54, 1179-1205.

Slomp, C.P., Van der Gaast, S.J., Van Raaphorst, W., 1996b. Phosphorus binding by poorly crystalline iron oxides in North Sea sediments. Mar. Chem. 52, 55-73.

Van Santvoort, P.J.M., De Lange, G.J., Thomson, J., Colley, S., Meysman, F.J.R., Slomp, C.P., 2002. Oxidation and origin of organic matter in surficial Eastern Mediterranean hemipelagic sediments. Aquat. Geochem. 8, 153-175.

Williams, J.D.H., Mayer, T., Nriago, J.O., 1980. Extractability of phosphorus from phosphate minerals common in soils and sediments. Soil Sci. Soc. Am. J. 44.

Table 1. Overview of the sequential chemical iron and phosphorus fractionation methods used in this study.

Step	Extractant, extraction time	Target phase	Name
	Fe fractionation		
1	1 mol L^{-1} Na acetate (buffered to pH 4.5 with acetic acid), 24 h	Carbonate-associated Fe	Fe_{carb}
2	1 mol L^{-1} hydroxylamine–HCl (in 25% v/v acetic acid), 24 h	Amorphous Fe (oxyhydr)oxides (ferrihydrite)	Fe_{ox1}
3	50 g L^{-1} Na dithionite (buffered to pH 4.8 with acetic acid/Na citrate), 2 h	Crystalline Fe oxides (goethite, hematite)	Fe_{ox2}
4	0.2 mol L^{-1} ammonium oxalate / 0.17 mol L^{-1} oxalic acid, 6 h	Recalcitrant Fe oxides (mostly magnetite)	Fe_{ox3}
	P fractionation		
1	1 mol L^{-1} $MgCl_2$, 30 min	Exchangeable P	P_{exch}
2*	25 g L^{-1} Na dithionite (buffered to pH 7.3 with Na citrate/Na bicarbonate), 8 h	Fe-associated P	P_{Fe}
3*	1 mol L^{-1} sodium acetate solution (buffered to pH 4 with acetic acid), 6 h	P in authigenic and biogenic Ca-P minerals and $CaCO_3$	P_{authi}
4	1 mol L^{-1} HCl, 24 h	Detrital P	P_{det}
5	ash at 550 °C (2 h), then 1 mol L^{-1} HCl, 24 h	Organic P	P_{org}

* These steps were followed by a wash step with 1 mol L^{-1} $MgCl_2$. The P extracted in this wash step was added to the total P extracted during that step.

Table 2. Position, water depth, bottom water dissolved oxygen concentrations and total organic C (C_{org}) and total P (P_{tot}) concentrations (core averages) for Station 1B and Station 2. The standard deviation is given in parentheses.

Station	latitude	longitude	water depth (m)	dissolved O_2 (µmol L^{-1})	C_{org} (wt%)	P_{tot} (µmol g^{-1})
1B	22°32.9’	64°02.4’	885	2.1	6.6 (± 0.9)	47 (± 8)
2	22°33.9’	64°03.8’	1013	2.9	3.7 (± 0.7)	46 (± 16)

Table 3. Source of all phosphorus reference materials analyzed with XANES spectroscopy in this study.

Reference materials	Source (DMC = Dartmouth Mineral Collection)
Ca-P minerals	
Collophane[a]	DMC, Florida, USA
Fluorapatite[a]	DMC (originally obtained from Harvard Museum Collection),
Apatite[a]	DMC, Gatineau National Park, Ottawa, Canada
Hydroxyapatite[a]	DMC, Bamle, Norway
Ca-phosphate tribasic	Commercial, Sigma-Aldrich
Cod bone	Cleaned, dried and ground fresh bones of cod fish
Ca-phosphate (amorphous)	Fresh precipitate of 0.001 mol L^{-1} Ca solution with a slight excess of dibasic phosphate. Resulting gel filtered with 0.2 micron filter.
Fe-associated P compounds	
Ferrihydrite-PO_4^{3-}	Ferrihydrite precipitated from $FeCl_3$ solution brought to pH 7 in the presence of PO_4^{3-} (filtered with 0.2 micron filter).
Strengite	DMC, Shady, Arkansas, USA
Beraunite	DMC, Shady Arkansas, USA
Vivianite	DMC, Richmond, Virginia, USA
Al-P compounds	
Variscite	DMC, Minas Gerais, Brazil
Lazulite	DMC, Graves Mountain, Georgia, USA (in quartzite)
Brazilianite	DMC, Newport, New Hampshire, USA
Wavellite	DMC, Pencil Bluff, Arkansas, USA
Various	
Phytic acid	Natural phytic acid (from soy).
Monazite	DMC, Columbia River, USA
Pyromorphite	DMC, Nassau, Germany
Na pyrophosphate (hydrated)	Commercial, Fisher Scientific
Pyrophosphate	Commercial, Fisher Scientific
Na polyphosphate	Commercial, Cascade detergent (~ 7.5 wt% P as $Na_5P_3O_{10}$)

[a] These are sedimentary Ca-P minerals where PO_4 groups in the mineral structure have been exchanged for carbonate (CO_3) to an unknown extent.

Table 4. Selected phosphorus reference materials used for least squares – linear combination fitting of sample XANES spectra. Formula represent general composition and not chemically determined elemental abundances.

Reference materials	Formula	Source (DMC = Dartmouth Mineral Collection)
Collophane	$Ca_5(PO_4,CO_3)_3F$	DMC, Florida, USA
Fluorapatite	$Ca_5(PO_4,CO_3)_3F$	DMC (obtained from Harvard Museum Collection), Greenwood, USA
Ferrihydrite-PO_4^{3-}	$Fe^{3+}(OOH)(PO_4)$	Ferrihydrite precipitated from $FeCl_3$ solution at pH 7 in the presence of PO_4^{3-}
Vivianite	$(Fe^{2+})_3(PO_4)_2$	DMC, Richmond, Virginia, USA
Na polyphosphate (pentasodium tri-phosphate)	$Na_5P_3O_{10}$	Commercial powdered sodium polyphosphate
Phytic acid	$C_6H_{18}O_{24}P_6$	Commercial phytic acid in aqueous solution (50:50)

Table 5. Results of P K-edge XANES analyses, including R-factor as indicator of goodness-of-fit.

Sample	Fe-associated P	Ca-P	organic P	R-factor
PA1B 0.25	0.63	0.17	0.11	0.0028
PA1B 1.75	0.54	0.10	0.29	0.0024
PA1B 4.5	0.65	0.00	0.15	0.0038
PA1B 11	0.11	0.39	0.41	0.0029
PA1B 22	0.17	0.46	0.12	0.0031
PA2 0.25	0.06	0.42	0.42	0.0009
PA2 6.5	0.06	0.56	0.30	0.0029
PA2 13	0.04	0.67	0.17	0.0007
PA2 26	0.00	0.50	0.41	0.0033

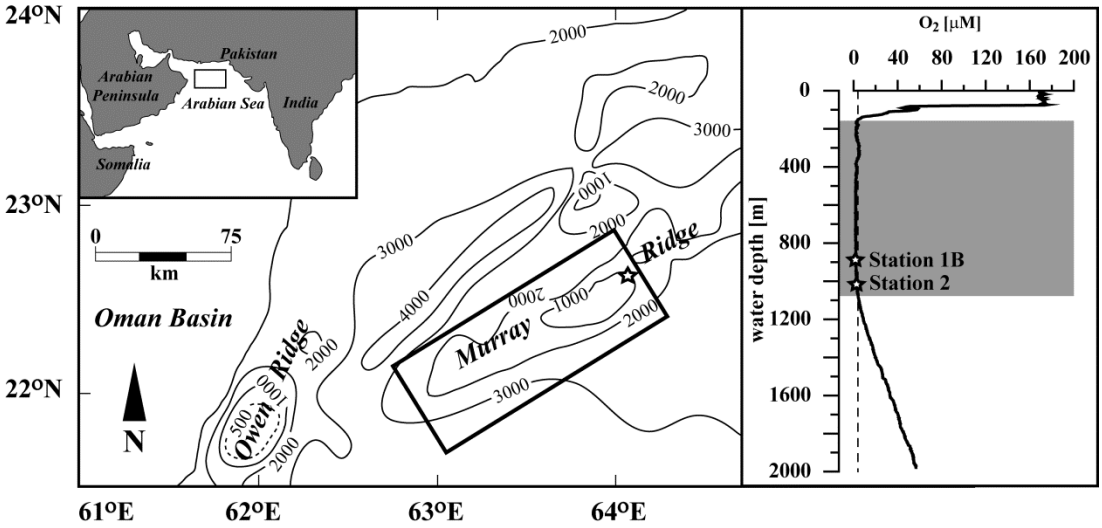

Fig. 1. Left panel: bathymetric map of the Arabian Sea with the location of the Murray Ridge study area indicated with a rectangle. The star symbol indicates approximate location of stations 1B and 2. Inset shows general regional geography. Taken from Kraal et al. (2012). Right panel: dissolved O_2 profile against water depth, stations indicated with star symbols and station number. Grey area in right panel indicates the oxygen minimum zone (OMZ) with dissolved $O_2 < 4.5$ µmol L^{-1}.

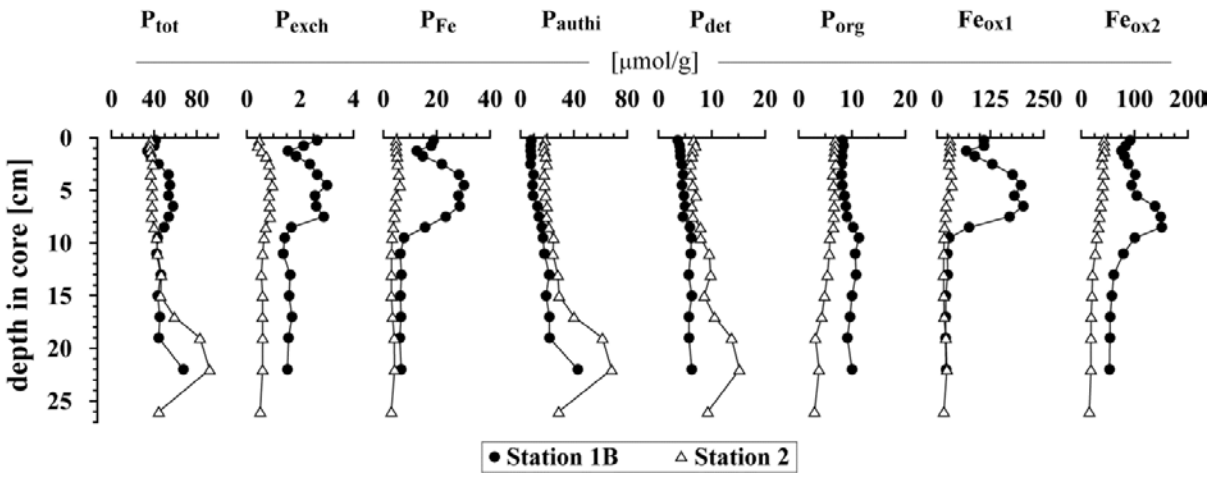

Fig. 2. Selected P and Fe fractions in sediments from sites 1B and 2: Concentrations of solid-phase total P and exchangeable P (P_{exch}), Fe-bound P (P_{Fe}), authigenic Ca-P (P_{authi}), detrital P (P_{det}) and organic P (P_{org}), and amorphous Fe (oxyhydr)oxides (Fe_{ox1}) and crystalline Fe oxides (Fe_{ox2}).

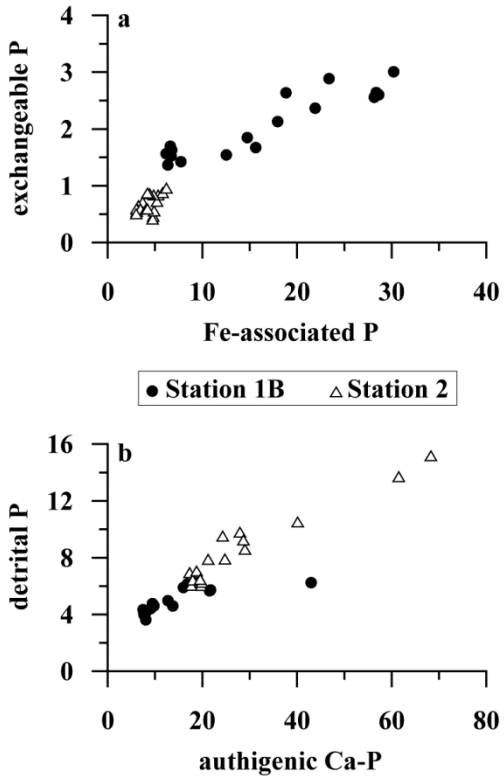

Fig. 3. Scatter plots of P species as determined by SEDEX: exchangeable P against Fe-associated P (a) and detrital P against authigenic Ca-P (b). All concentrations are in µmol g^{-1}.

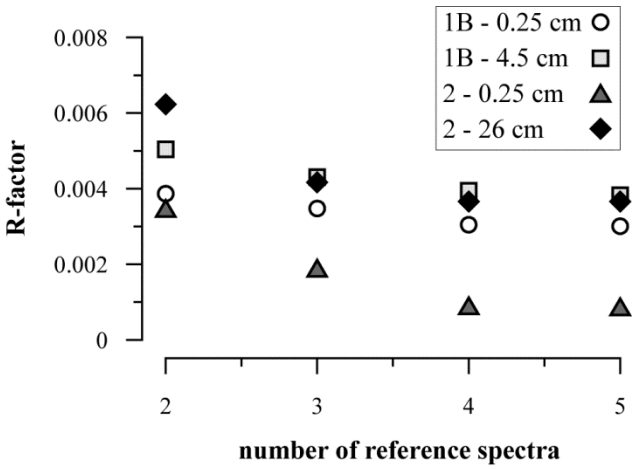

Fig. 4. Goodness-of-fit (R-factor) plotted against number of reference materials for four representative sample XANES spectra. R-factor values represent the average of the three best fits for the corresponding number of reference spectra.

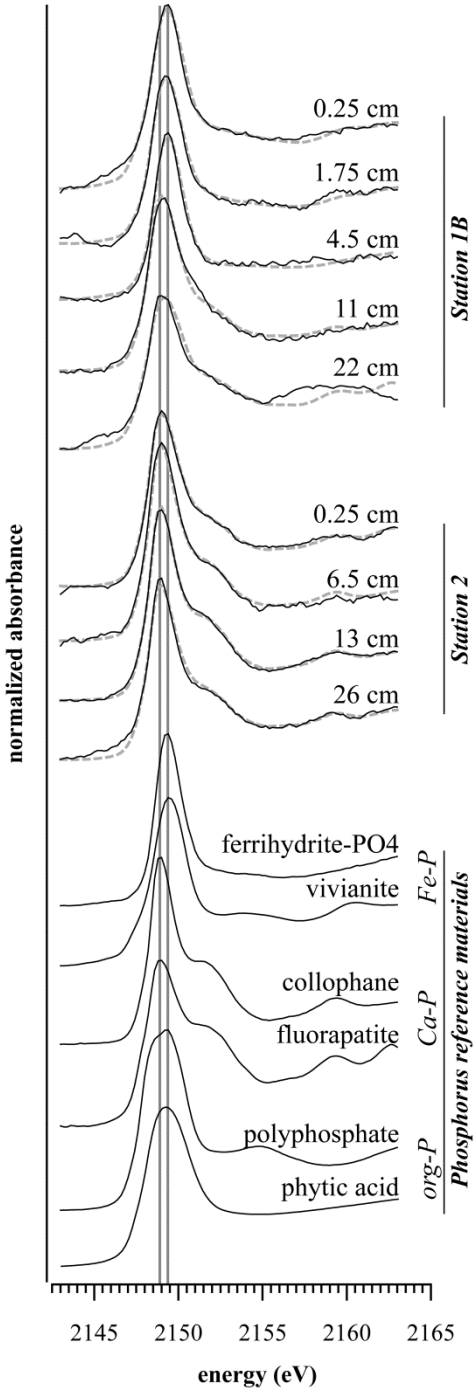

Fig. 5. Phosphorus K-edge XANES spectra of samples from station 1B (top) and 2 (middle), and phosphorus reference materials (bottom). Solid black lines show data, dashed grey lines for sample spectra show LCF model fits. Vertical solid grey lines are centered at absorbance peaks for Fe-associated P and Ca-P reference materials.

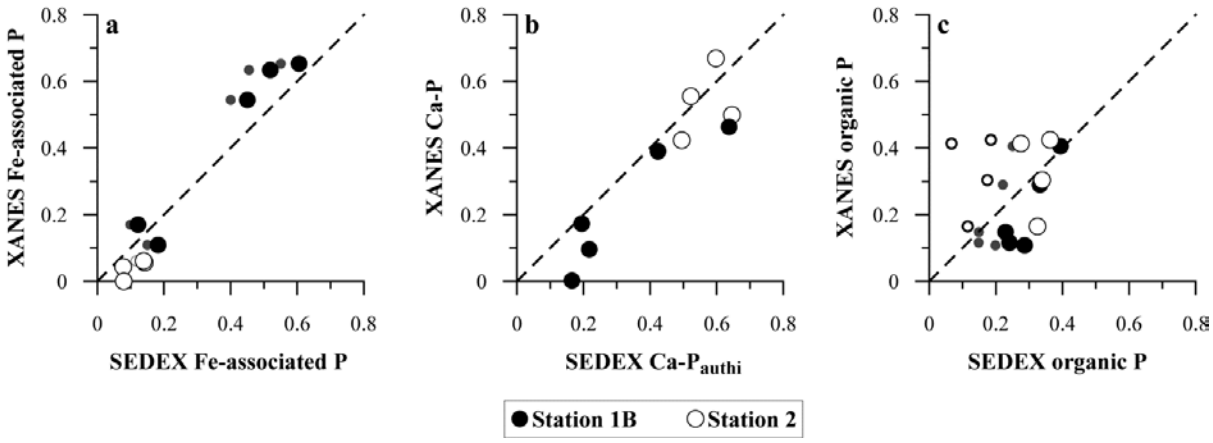

Fig. 6. Scatter plots of phosphorus species Fe-associated P (a), Ca-P (b) and organic P (c) as determined by SEDEX sequential extraction and P K-edge XANES spectroscopy. In (a), small symbols represent SEDEX Fe-associated P and large symbols represent the sum of SEDEX Fe-associated P and exchangeable P. In (c), small symbols represent SEDEX organic P and large symbols represent the sum of SEDEX organic P and detrital P. Dashed diagonal lines in all plots show a 1:1 relationship.

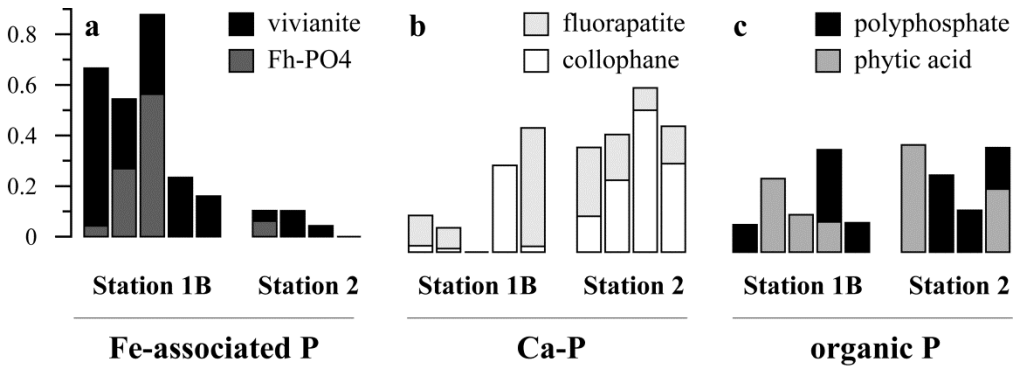

Fig. 7. Bar chart showing relative contribution of individual reference materials to the major P species Fe-associated P (a), Ca-P (b) and organic P (c), as determined by P K-edge XANES spectroscopy.